RSC Advances

PAPER

View Article Online
View Journal | View Issue

Cite this: *RSC Adv.*, 2025, **15**, 39962

Biobased diblock copolymers and associated reactivity ratios *via* RAFT-polymerisation as new dispersing additives

Lea Viktoria Rubbert,*[a] Philipp Knospe,[b] Sebastian Weiß,[b] Maximilian Scherübl,[b] Lukas Wander,[b] Jochen S. Gutmann[c] and Michael Dornbusch[a]

Diblock copolymers with structural heterogeneity, made of monomers based on renewable resources were investigated as dispersing additives for nonpolar coating systems. Reversible addition–fragmentation transfer (RAFT) polymerisation was used to obtain (diblock co)polymers with tailor-made structures and molecular weights M_w. For this purpose methacrylates derived from oleyl alcohol and eugenol, were utilized. The reaction kinetics of controlled and free radical polymerisation processes for methacrylated eugenol (4-allyl-2-methoxyphenyl methacrylate) (**1**) and methacrylated oleyl alcohol (octadec-9-en-1-yl methacrylate) (**2**) were investigated. In addition, commercially available methacrylates – including methyl methacrylate (**3**), methacrylic acid (**4**), benzyl methacrylate (**5**) and stearyl methacrylate (**6**) were used for building diblock copolymers. Reaction kinetics of the homopolymers **3** and **6** were compared to those of methacrylates **1** and **2**. By RAFT-Polymerisation of Methacrylate **1**, pronounced cross-linking was observed, suggesting the active participation of the allyl group. Subsequent investigations confirmed that the allyl group underwent partial conversion. By lowering the concentration, the cross-linking reaction could be minimized, enabling the synthesis of diblock copolymers. Finally, their performance as dispersing additives was evaluated in non-polar coating systems containing inorganic and carbon black pigments. To measure performance, properties such as rheological behavior and particle size distribution were analysed. All diblock copolymers showed good dispersity properties for all pigments, with particularly pronounced effects for the fully bio-based block copolymer **poly(2-*b*-4)** and the partially bio-based block copolymer **poly(6-*b*-1)**.

Received 11th September 2025
Accepted 13th October 2025

DOI: 10.1039/d5ra06866e

rsc.li/rsc-advances

Introduction

Over the past decades, the chemical industry has undergone a significant shift in raw material utilization.[1–3] The study of natural products has expanded the range of viable raw materials, including sugar, starch, cellulose, and natural fats and oils, presenting promising opportunities for sustainable development.[4–10] This trend is particularly evident in the production of specialty chemicals, where product portfolios are being adapted to integrate renewable raw materials, replacing conventional fossil-based products whenever feasible.[11–13] However, these new formulations must still meet the high-performance requirements and align with customer expectations.[14,15] Polymers have become indispensable in modern daily life and are widely used in various materials.[16–19] They are utilized as efficient emulsifiers,[20] rheology modifier,[21] drug delivery agents,[22–24] nano particle[21,25] and much more.[26] Tailor-made polymers serve a pivotal function in the paints and coatings sector as advanced functional additives.[4,14] Additives are crucial components in paint formulations, influencing multiple stages even in minimal concentrations.[27] One of the primary challenges for paint formulators is the stabilisation of pigments and preventing them from reagglomeration during the grinding process. For this purpose nanoparticles or polymer structures can be used. Among various polymer architectures, tailor-made diblock copolymers have gained considerable attention due to their strong interactions with pigment surfaces, ensuring effective stabilization across diverse media.[27] Advancements in controlled radical polymerisation (CRP) techniques have enabled the synthesis of highly specialized additives that outperform conventional dispersing agents by offering superior application properties and narrow molecular weight distributions. Structural heterogeneous block copolymers have emerged as promising pigment dispersants, owing to their possibility of self-assembling: the hydrophobic part ensures steric stabilization, while the hydrophilic domain enhances dispersion stability through strong pigment affinity.[14] Reversible addition–fragmentation transfer (RAFT) polymerisation provides precise control over molecular weight and enables the polymerisation of

[a]*Hochschule Niederrhein University of Applied Sciences, ILOC-Institute, Krefeld, Germany. E-mail: viktoria.rubbert@altana.com*
[b]*BYK-Chemie GmbH, Wesel, Germany*
[c]*Group of Physical Chemistry, University of Duisburg-Essen, Essen, Germany*

a diverse range of monomers.[3,28,29] First introduced in 1998, this controlled radical polymerisation (CRP) technique has evolved into one of the most versatile and powerful methods for synthesizing complex polymer architectures.[30] The use of iniferter reagents (initiator–transfer agent–terminator)[31] facilitates a controlled equilibrium between active and persistent radicals, ensuring a well-regulated initiation process and reversible chain termination. This approach is classified as reversible deactivated radical polymerisation (RDRP).[32] RAFT polymerisation represents a subclass of RDRP, wherein chain propagation is precisely controlled *via* Chain Transfer Agents (CTA).[33–35] Today, increasing commercial availability of these agents has gained industrial interest in RAFT polymerisation. This technique is highly adaptable for producing polymers with narrow dispersities and tailored architectures. By carefully selecting CTAs and optimising reaction conditions, superior results in control of molecular weight and dispersity can be obtained for most monomers compared to free radical polymerisation.[35] The precise linkage of highly dissimilar monomers into structurally heterogeneous copolymers—often elusive *via* conventional polymerisation routes—can be effectively achieved using RAFT polymerisation.[14,24,36,37] Eugenol is the primary component of clove oil, with approximately 90% of its composition. It is further well known for its analgesic and antiseptic properties.[2,38] The incorporation of additional functional groups through the hydroxyl functionality allows the design of a highly reactive monomer.[15,39] Oleyl alcohol is commonly synthesized by hydrogenating oleic acid esters. It is derived from rapeseed oil and is a versatile raw material which can be used as non-ionic surfactant, emulsifier, plasticizer, and thickener.[5] Additionally, its terminal hydroxyl group can be converted to polymerizable groups, such as methacrylates. The attachment of methacrylate groups to both phenolic and non-phenolic hydroxyl functionalities is achieved *via* a Steglich esterification reaction using methacrylic anhydride.[15] The aim of this study was the synthesis of tailored diblock copolymers, including the use of monomers based on renewable raw materials, for application as dispersing additives in nonpolar systems. To establish the fundamental synthesis of structurally heterogeneous diblock copolymers, **poly(6-*b*-3)** was initially synthesised *via* RAFT polymerisation with a block ratio of 1 : 1 and a molecular weight of 5000 g per mol per block.

For application as dispersing additives, the copolymers **poly(6-*b*-3)**, **poly(2-*b*-3)**, **poly(6-*b*-1)**, **poly(2-*b*-1)**, and **poly(6-*b*-5)** were synthesised with a block length ratio of 1 : 3, corresponding to molecular weights of 7500 g mol^{-1} and 2500 g mol^{-1}, respectively. Additionally, all homopolymers corresponding to these copolymers were prepared. This molecular weight was chosen because the application as a dispersing additive typically requires polymers within this molecular weight range to ensure optimal stabilisation.

Experimental

Materials

Eugenol (>99%, Carl Roth), oleyl alcohol (>99% Sigma-Aldrich), methacrylic anhydride (contains 2000 ppm topanol A as inhibitor, >94%, Sigma-Aldrich), dimethyl aminopyridine (>99%, Carl Roth), ethyl acetate (>95%, Carl Roth), sodium hydrogen carbonate (>99,5%, Carl Roth), basic aluminium oxide (>99%, Carl Roth), magnesium sulfate (anhydrous, ReagentPlus®, ≥99.5%, Sigma-Aldrich), Exxol D100 (>95%, Univar Solutions), ethyl hexyl cocoat (>98, Oleon GmbH) and 4-cyano-4-(((dodecylthio)carbonothioyl)thio)pentanoic acid (97%, BORON MOLECULAR), Azodi(2-methylbutyronitrile (98%, Sigma-Aldrich)) were used as received. Methyl methacrylate (contains ≤30 ppm MEHQ as inhibitor, 99%, Sigma-Aldrich), stearyl methacrylate (mixture of stearyl and cetyl methacrylates, contains MEHQ as inhibitor, Sigma-Aldrich), benzyl methacrylate (96%, contains monomethyl ether hydroquinone as inhibitor, Sigma-Aldrich), methacrylic acid (contains 250 ppm MEHQ as inhibitor, 99%, Sigma-Aldrich) and methoxy propyl acetate (>95%, Sigma-Aldrich) were purged with nitrogen and kept under it.

Synthesise of monomers derived from eugenol and oleyl alcohol

Methacrylates **1** and **2** (Fig. 1) were synthesized by the esterification reaction with eugenol and oleyl alcohol with methacrylic anhydride. This process involves homogenizing methacrylic anhydride with the target compound in the presence of a catalyst, maintaining the reaction for at least 24 hours at approximately 45 °C. The methacrylic acid formed during the reaction can be captured using a basic component, improving the efficiency of the synthesis.[6] Firstly, 32 mmol eugenol or oleyl alcohol, 48 mmol methacrylic anhydride and 0.66 mmol dimethyl aminopyridine (DMAP) were added into a 250 mL flask and homogenised in 15 mL ethyl acetate. Secondly, 72 mmol sodium bicarbonate was dissolved in 81.25 mL deionized water and added to the reaction mixture. The two-phased system was subjected to emulsification through the implementation of vigorous stirring for more than 24 h at RT. After 24 hours, the aqueous phase was removed, and freshly saturated sodium hydrogen carbonate solution was added. Subsequently the solution was diluted with 100 mL ethyl acetate and the aqueous phase were removed. The organic layer was sequentially washed with deionized water. The final product as obtained after drying over $MgSO_4$, filtering with basic aluminium oxide, rotary evaporation and drying in a vacuum. The final product was obtained as a clear liquid with conversions >90%. The synthesized monomers were analysed using ^{1}H-NMR and (Fig. S1 and S2) FT-IR spectroscopy (Fig. S45 and S46).

Synthesise of tailor-made RAFT-homopolymers

Homopolymers using methyl methacrylate (**3**) stearyl methacrylate (**6**), benzyl methacrylate (**5**), methacrylic acid (**4**) and methacrylate **1** and methacrylate **2** were synthesized (Scheme 1). For this purpose, 30 wt% of monomer, 4-cyano-4-(((dodecylthio) carbonothioyl)thio)pentanoic acid (**CTA-1**) and azodi(2-methylbutyronitrile) (AMBN) were dissolved in methoxy propyl acetate (PMA). Used were a ratio [CTA] : [AMBN] = 3 and an amount [CTA] : [monomer] was calculated according to the targeted molecular weight for the polymers. Meanwhile, the remaining monomer were purged with nitrogen gas for 20

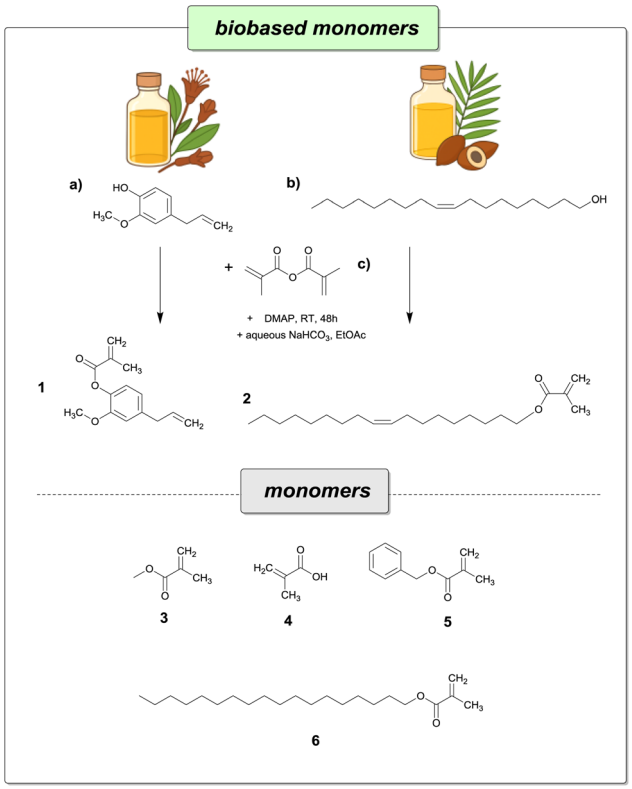

Fig. 1 Chemical structures of the raw materials and methacrylates (a) eugenol, (b) oleyl alcohol, (c) methacrylic anhydride, (**1**) 4-allyl-2-methoxy-phenyl methacrylate, (**2**) Octadec-9-en-1-yl methacrylate, (**3**) methyl methacrylate, (**4**) methacrylic acid, (**5**) benzyl methacrylate, (**6**) stearyl methacrylate.

minutes. The reaction mixture was continuously stirred with nitrogen throughout the entire duration of the reaction. Following the heating of the initial reaction mixture to 75 °C, the remaining amount of monomer was added over a period of two hours. The reaction was terminated after monomer conversion >98%, monitored by ^{1}H NMR spectroscopy. The synthesized polymers were precipitated in methanol or *n*-hexene and characterized using ^{1}H-NMR (Fig. S3–S8, S15 and S16), GPC (Fig. S17–S24), DSC (Fig. S31–S37), TGA (Fig. S44) and FT-IR spectroscopy (Fig. S45–S51 and S53–S55).

Synthesise of tailor-made RAFT-diblock copolymers

The A-block was synthesized as described above. The block copolymer was prepared *via* a one-pot reaction by directly extending the A-block. After achieving 95–98% conversion, monitored by ^{1}H NMR spectroscopy, the second monomer was purged with nitrogen added to the corresponding first block over a period of two hours. After 2 hours, initial amount AMBN was added. The reaction was also terminated after monomer conversion >98%, monitored by ^{1}H NMR spectroscopy. The synthesized polymers were precipitated in methanol and characterized using ^{1}H-NMR (Fig. S9–S14), GPC (Fig. S25–S30), DSC (Fig. S38–S43), TGA (Fig. 8) and FT-IR spectroscopy (Fig. S52 and 7).

Application of synthesised block copolymers as dispersing additive in nonpolar system

The new block copolymers were employed as dispersing agents in nonpolar formulations containing inorganic pigment or carbon black. 77.5 wt% Exxol D 100, 7.5 wt% dispersant and 15 wt% carbon black were combined. 50.2 wt% ethylhexyl cocoate, 5.3 wt% dispersant and 44.5 wt% inorganic pigment were also blended. An equal amount regarding the formulations of milling beads was added to the solvent, dispersant, and pigment, and the mixtures were placed on a shaker for 16 hours. Subsequently, viscosity and particle size were measured. The samples were then stored at 60 °C for an additional two weeks. Viscosity and particle size were re-evaluated after storage.

Characterization

Nuclear magnetic resonance spectroscopy (NMR). Chemical structure of MDE and MOA and monomer conversions were determined by ^{1}H-NMR with a Bruker Avance 500 MHz spectrometer at 295 K. Spectra were recorded by dissolving sample in $CDCl_3$ and/or DMSO-D6. TMS (tetramethyl silane) was used as internal standard. The conversions were calculated by monitoring of the methacrylate double bond.

Additionally, DOSY measurements were performed using the pulse program stebpgpls with a gradient strength (gpz6) of 100%, a diffusion time (*d*20) of 0.1 seconds, and a temperature of 295 K in $CDCl_3$. Furthermore, ^{1}H-NMR spectra were acquired with diffusion filtering applied at 98% gradient strength to suppress low-diffusing components.

A Spinsolve 80 MHz ULTRA (Magritek GmbH, Aachen Germany) Benchtop spectrometer was used for monitoring the reactions kinetics.

Thermogravimetric analysis (TGA). Thermogravimetric analysis was conducted using a TGA Q5000 IR apparatus from TA instruments, with a temperature range of 20 to 300 °C and a heating rate of 10 K min^{-1} under an air atmosphere. Samples

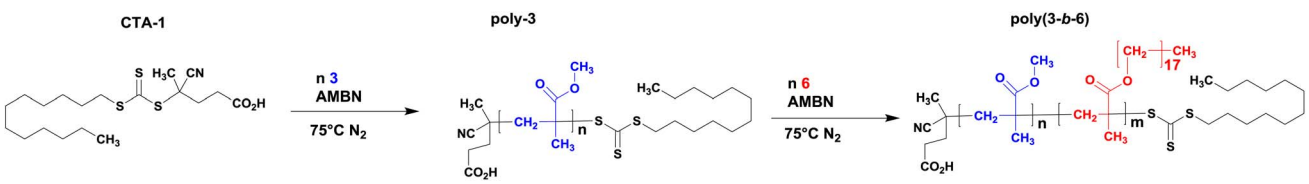

Scheme 1 Systematic representation of the polymerisation of methacrylate **3** using **CTA-1**, initiated by AMBN at a temperature of 75 °C. In the second step, methacrylate **6** was polymerized to form the block copolymer **poly(3-*b*-6)**.

were prepared in a platinum pan, using 10–100 mg of polymer. The Thermal Decomposition Temperature (T_D) was determined accordingly.

Differential scanning calorimetry (DSC). DSC measurements were performed under nitrogen atmosphere using the DSC Q2000 apparatus from TA instruments. Sample were prepared in an aluminium pan and measured using the following heating/cooling cycles: first heating ramp from −80 °C or 20 °C to 140 °C at 10 K min^{-1}, isotherm plateau at 140 °C for 3 min, cooling ramp from 140 °C to 20 °C, isotherm plateau at 20 °C for 3 min and second heating ramp from −80 °C or 20 °C to 140 °C. Glass transition temperature (T_g) or melting point (T_m) values are given from the evaluation of the second heating ramp.

Gel permeation chromatography (GPC). Molecular weight distribution of polymers was determined by gel permeation chromatography using separation module, equipped with Refractive Index Detector waters 2695 and a combination of three HR styragel columns (pore size: 5.7 μm, 7.8 mm × 300 mm). Tetrahydrofuran (THF) was used as an eluant. A polystyrene standard (Mp: 1 000 000–162) was used for calibration.

Fourier transform infrared spectroscopy (FTIR). FTIR characterization was recorded on a Thermo Scientific Nicolet-FT-IR Spectrometer iS10 with a resolution of 0.4 cm^{-1}.

Viscosity measurements. Rheological measurements were measured using Rheometer MCR 301 from Anton Paar with cone and plate geometry (25 mm/4° angle) at temperature 25 °C. The viscosities were analysed at shear rate 100 1 s^{-1}.

Particle size measurement. Particle size measurements were recorded using a Zetasizer Advance Series Pro (blue) from Malvern.

Estimation of kinetic parameters

To estimate the reactivity data, it was assumed that the RAFT polymerisations follow pseudo-first-order kinetics, while the free-radical polymerisations follow zero-order kinetics.[3,35,40,41] For pseudo-first-order, kinetic plots of $\ln[M]_0/\ln[M]_t$ *versus* time were constructed. For zero-order kinetics, plots of $1/[M]_t$ *versus* time were used. In both cases, linear regressions were performed starting from the first measurable monomer conversion. The reaction rate constant k was determined from the slope of the linear regression.

Results and discussion

Synthesis of monomers derived from eugenol and oleyl alcohol

Several synthetic approaches for the functionalization of eugenol and oleyl alcohol with methacrylate groups have been reported in literature.[15,42,43] Methacrylation *via* Steglich esterification using methacrylic anhydride under catalytic conditions offers significant advantages over conventional methods, due to its mild reaction environment, high product yields, and reduced formation of side products.[15] One of the principal benefits of the synthetic strategy adopted in this study is the *in situ* removal of methacrylic acid generated during the reaction, which enhances conversion rates and minimizes side reactions. Conventional methodologies for eliminating methacrylic acid from the reaction mixture, as reported in the literature, often involve the addition of triethylamine (TEA) or thermal treatment.[3,15] However, these strategies present significant drawbacks: the formation of undesirable by-products such as oligomers and environmental concerns associated with TEA usage. Additionally, traditional processes necessitate laborious, multi-step purification protocols. During this study, a novel method was developed where methacrylic acid selectively emulsified into a mildly basic aqueous phase, followed by phase separation. This streamlined approach markedly simplifies purification, by requiring only few sequential aqueous washing steps to achieve high reaction yields (>98%) and exceptional product purity.

Reaction kinetics of various methacrylates *via* RAFT polymerisation

The homopolymerisations (Table 1) resulted in uniform chain growth (Fig. 3) with low dispersity. The targeted molecular weights were closely achieved for all homopolymers *via* RAFT polymerisation. Conversions exceeding 98% were obtained by subsequent addition of AMBN, which led to the reactivation of dormant chains. This re-initiation had no observable effect on

Table 1 Overview of concentration of reaction solution in PMA, conversion percentage (conv. %), theoretical molecular weight ($M_{n,th}$), actual molecular weight (M_n) and dispersity M_w/M_n and glass transition temperature (T_g), melting point (T_m), and thermal decomposition temperature (T_D)

Polymer	[M] (mol L^{-1})	Conv. (%)	$M_{n,th}$, (g mol^{-2})	M_n (g mol^{-2})	M_w/M_n	T_m (°C)	T_g (°C)	T_D (°C)
poly-3	7.3	99	5000	4200	1.1	—	85.7	159.3
poly-1	0.8	85	5000	4400	1.8	—	94.6	158.4
poly-4[b]	8.5	95	5000	5300	1.1	—	—[c]	120.0
poly-5	3.3	99	5000	4660	1.2	—	−21.9	115.5
poly-6	7.3	99	5000	5500	1.2	33.8	110.0	180.1
poly-2	7.3	88	5000	4200	1.4	—	103.6	169.4
poly-1[a]	0.8	89	—	11 800	5.9	—	116.5	163.4
poly-2[a]	7.3	72	—	5030	1.8	—	107.7	177.7

[a] Free radical polymerisation. [b] Synthesized in DMSO. [c] Measurement not possible, as T_g is above T_D for RAFT polymer.

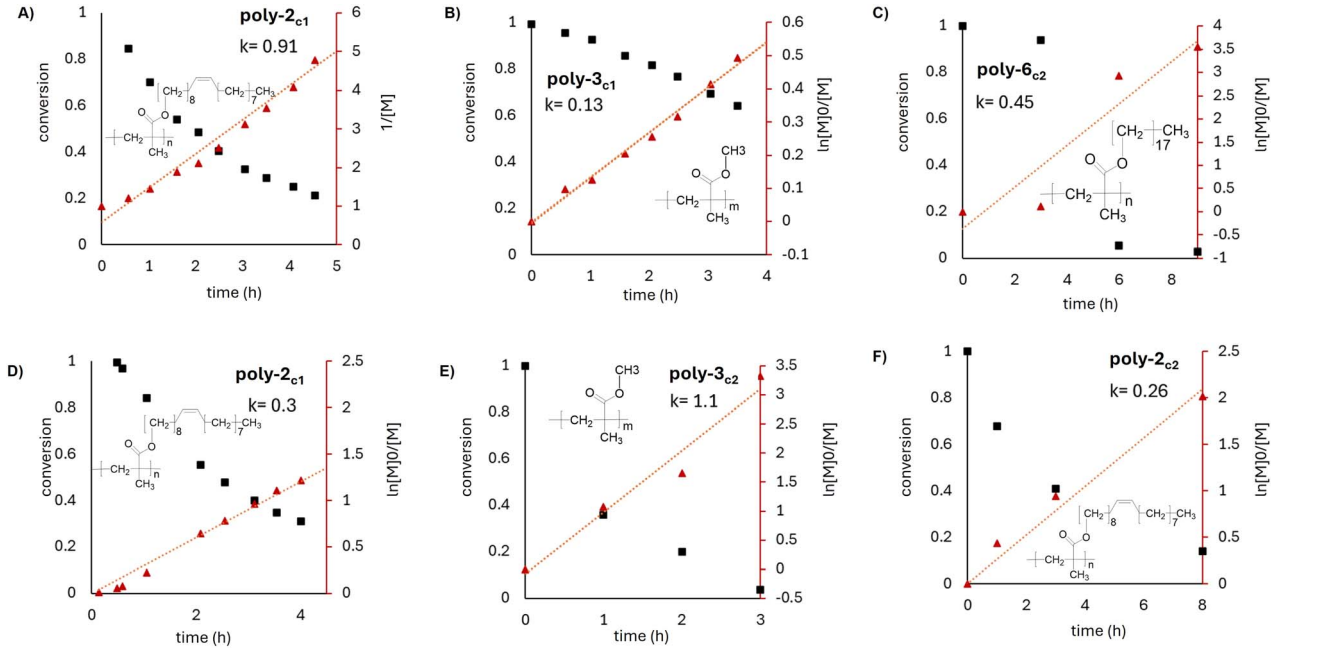

Fig. 2 (A) Free radical polymerisation of **poly-2** ([*M*] = 0.8 mol L^{-1}), conversion over time and 1/[*M*] over time, assuming 0. Order kinetics/(B) RAFT polymerisation of **poly-3** ([*M*] = 0.8 mol L^{-1}) conversion over time and $\ln[M]_0/[M]$ over time, assuming pseudo-first-order/(C) RAFT polymerisation of **poly-6** ([*M*] = 7.3 mol L^{-1}) conversion over time and $\ln[M]_0/[M]$ over time, assuming pseudo-first-order kinetics/(D) RAFT polymerisation of **poly-2** ([*M*] = 0.8 mol L^{-1}) conversion over time and $\ln[M]_0/[M]$ over time, assuming pseudo-first-order kinetics/(E) RAFT polymerisation of **poly-3** ([*M*] = 7.3 mol L^{-1}) conversion over time and $\ln[M]_0/[M]$ over time, assuming pseudo-first-order/(F) RAFT polymerisation of **poly-2** ([*M*] = 7.3 mol L^{-1}) conversion over time and $\ln[M]_0/[M]$ over time, assuming pseudo-first-order kinetics.

the dispersity. Additionally, monomer **1** and monomer **2** were polymerized *via* free-radical polymerisation. Remarkably, **poly-2** exhibited an unexpectedly low dispersity for a polymer synthesized through a free radical pathway, which may be attributed to self-stabilizing effects induced by its aliphatic chain. The reaction kinetics of monomer **2** were investigated under various reaction conditions (Fig. 2). Polymerisations were conducted at concentrations of c_1 (0.8 mol L^{-1}) and c_2 (7.3 mol L^{-1}). In addition, the kinetics of the free-radical polymerisation of monomer **2** were evaluated at a concentration of c = 0.8 mol L^{-1}. For comparison, the polymerisation kinetics of monomers **3** and **6** were also assessed. The reaction kinetics of monomer **3** were also examined at both concentrations. The polymerisation performed in a diluted system resulted in a substantially lower reaction rate constant for monomer **3** (Table 2). Lower monomer concentration leads to a slower reaction rate due to several factors: firstly, dilution effects on the equilibrium of reversible-deactivated radical polymerisation, shifting the balance between active and deactivated species.[40,41] Secondly, reduced collision frequency between monomer and initiator, resulting in a decreased propagation rate. Regarding polymerisation of **poly-6**, a significantly lower reaction rate was observed compared to **poly-3**. This result can be primarily attributed to steric hindrance, which is enhanced by the aliphatic chain structure, thereby reducing polymerisation

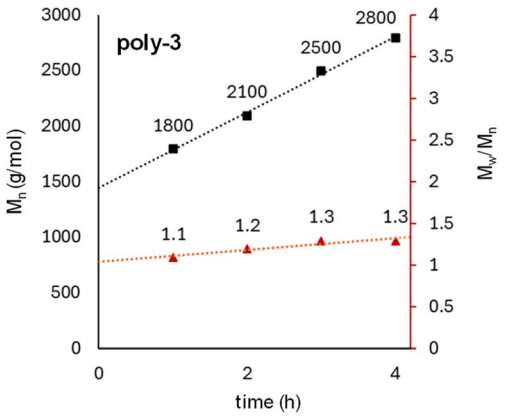

Fig. 3 Molecular weight and dispersity over time for **poly-3**.

Table 2 Overview of concentration of reaction solution in PMA and of evaluated kinetic rate constants[b]

Polymer	[*M*] mol L^{-1}	*k*	R^2
poly-1$_{c1}$	0.8	0.22	0.99
poly-2$_{c1}$	0.8	0.30	0.99
poly-2$_{c2}$	7.3	0.26	0.99
poly-3$_{c2}$	7.3	1.10	0.99
Poly-3$_{c1}$	0.8	0.13	0.95
poly-6$_{c2}$	7.3	0.45	0.88
poly-1$_{c1}$[a]	0.8	0.28	0.99
poly-2$_{c1}$[a]	0.8	0.91	0.97

[a] Free radical polymerisation. [b] Measurement not possible, as T_g is above T_D for RAFT polymer.

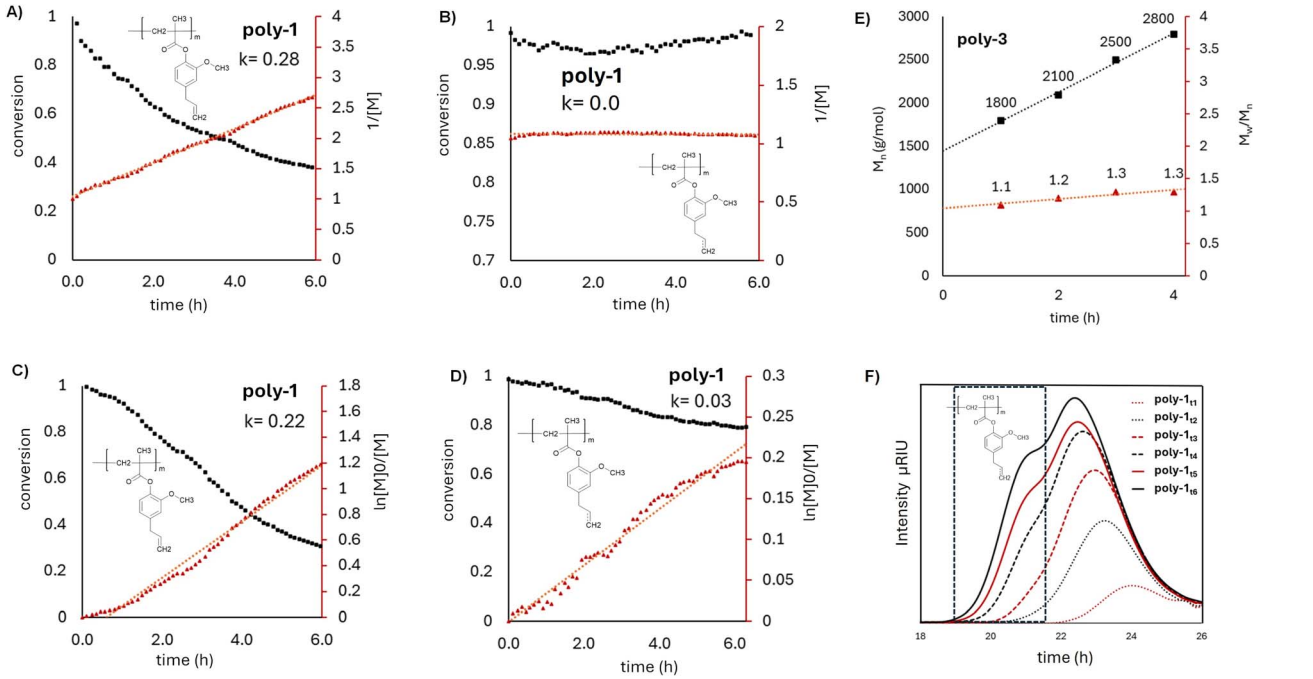

Fig. 4 (A) Free radical polymerisation of **poly-1** ([*M*] = 0.8 mol L^{-1}), conversion C=C double bond methacrylate over time and 1/[*M*] over time, assuming 0. Order kinetics/(B) free radical polymerisation of **poly-1** ([*M*] = 0.8 mol L^{-1}), conversion C=C double bond allyl group over time and 1/[*M*] over time, assuming 0. Order kinetics/(C) RAFT polymerisation of **poly-1** ([*M*] = 0.8 mol L^{-1}) conversion C=C double bond methacrylate over time and $\ln[M]_0/[M]$ over time, assuming pseudo-first-order kinetics/(D) RAFT polymerisation of **poly-1** ([*M*] = 0.8 mol L^{-1}) conversion C=C double bond allyl group over time and $\ln[M]_0/[M]$ over time, assuming pseudo-first-order kinetics/(E) molecular weight and dispersity over time for **poly-1** (F) GPC elugrams over increasing polymerisation conversion for **poly-1**.

efficiency. A similar steric effect was observed in the controlled polymerisation of **2**. A comparison of the reaction rate constants *k* for the polymerisation of **poly-2** at different concentrations reveals that the rate is higher at lower concentration. This observation contrasts with the results obtained for **poly-3**, but can be explained by considering that steric hindrance plays a smaller role under dilute conditions. Additionally, larger particle size can increase the likelihood of intermolecular collisions. Free radical polymerisation demonstrated a substantially higher polymerisation rate. This outcome is in line with the fundamental characteristics of free-radical polymerisation. Radicals initiate chain propagation with considerable efficiency, resulting in rapid monomer conversion. However, this accelerated reactivity comes at the expense of molecular weight control, often leading to polymers with a broad molecular weight distribution.[44] The thermal stability of the synthesized polymers by their thermal decomposition temperature (T_D) was determined (Table 1). The T_D values ranged from 115 °C to 180 °C. This range correlates with that of the CTA, for which a T_D of 163 °C was measured. This may indicate that, without further stabilization after cleavage of the CTA, degradation of the polymer chain is promoted. The aliphatic monomers exhibiting higher decomposition temperatures 180 °C for **poly-6** and 169 °C for **poly-2**. Monomer **6** exhibits semi-crystalline structures, further enhancing its thermal stability. This phenomenon was confirmed through Differential Scanning Calorimetry (DSC) analysis, where **poly-6** showed a glass transition temperature (T_g) of 110 °C (Table 1) and also a distinct melting and crystallization point of 33 °C, reinforcing its resilience under thermal stress. When comparing the measured T_g of **poly-3** (86 °C) produced *via* RAFT polymerisation with the value reported in the literature for **poly-3** (approximately 105 °C), it is notable that a significantly lower T_g was achieved.[45] This observation could be explained by that RAFT polymerisation enables precise control over polymer chain growth, resulting in well-defined molecular weight distributions and narrow dispersities. Additionally, due to the controlled nature of RAFT polymerisation, the resulting polymers often exhibit weaker intermolecular forces, particularly when polar groups are minimized. The reduced strength of dipolar and hydrogen bonding interactions lowers the rigidity of the polymer matrix, thereby facilitating chain mobility and reducing T_g.[45–47] A conversion of at least 85%, and in most cases above 95%, was achieved for all homopolymers. The targeted molecular weight of 5000 g mol^{-1} was nearly reached for all homopolymers, with dispersity values between 1.1 and 1.4 (Table 1). However, **poly-1** exhibited a dispersity of PDI = 1.8 at 85% conversion, which had been previously analysed and attributed to specific reaction kinetics.

Reactivity of the allyl group in eugenol during RAFT polymerisation

Special attention was given to the RAFT polymerisation of **poly-1**, as an unexpected strong crosslinking reaction was observed

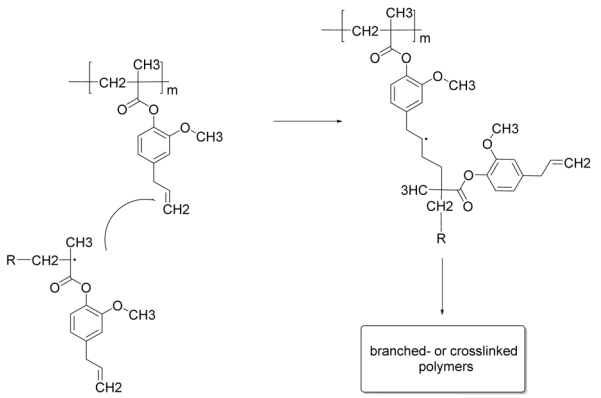

Scheme 2 Possible reaction between the propagating polymerisation species and the allyl group of **poly-1**.[48]

using c_2. By reducing the concentration to c_1, the crosslinking reaction could be suppressed, resulting in the formation of a fully soluble polymer. In contrast, no crosslinking was detected during the free-radical polymerisation of **poly-1**. To further investigate the cause of crosslinking, an online NMR analysis was conducted, tracking the conversion of the allyl C=C double bond and the methacrylate group for monomer **1** (Fig. 5). In RAFT polymerisation using **CTA-1**, which is primarily suited for MAM (more activated monomers), and the concentration of c_1, a significant conversion approximately 20% of the allyl group was observed, whereas the methacrylate group reacted to around 70% over the same time frame (Fig. 4C and D). These data clearly demonstrate the reactivity of the allyl double bond under the chosen conditions, even though reaction of methacrylate C=C double bond is preferred. In the free radical polymerisation, the allyl double bond remained entirely unaffected, with reaction occurring only at the methacrylate group (Fig. 4A and B). The reactivity of the allyl double bond in eugenol is sparsely documented in the literature. However, initial detailed studies have shown that activation of this functionality can occur through alternative controlled polymerisation methods, such as ATRP.[48] Electronic structure calculations support that monomer addition preferentially proceeds *via* the methacrylate group, although allyl group reactivity is also energetically accessible.[48] It is reported that the initiation step by the initiator radical preferentially occurs at the methacrylate moiety. Subsequently, the monomer radical exhibits a favoured reactivity toward the C=C double bond of the methacrylate, as this pathway is energetically favourable and proceeds without significant steric hindrance. In contrast, an attack on the allylic double bond leads to the formation of a secondary radical (Scheme 2), which lacks resonance stabilization, thereby requiring the system to overcome a higher activation energy barrier. Nevertheless, an attack of the propagating RAFT-initiated polymer chain on the allyl group is likely, which may lead to crosslinking reactions. High concentrations

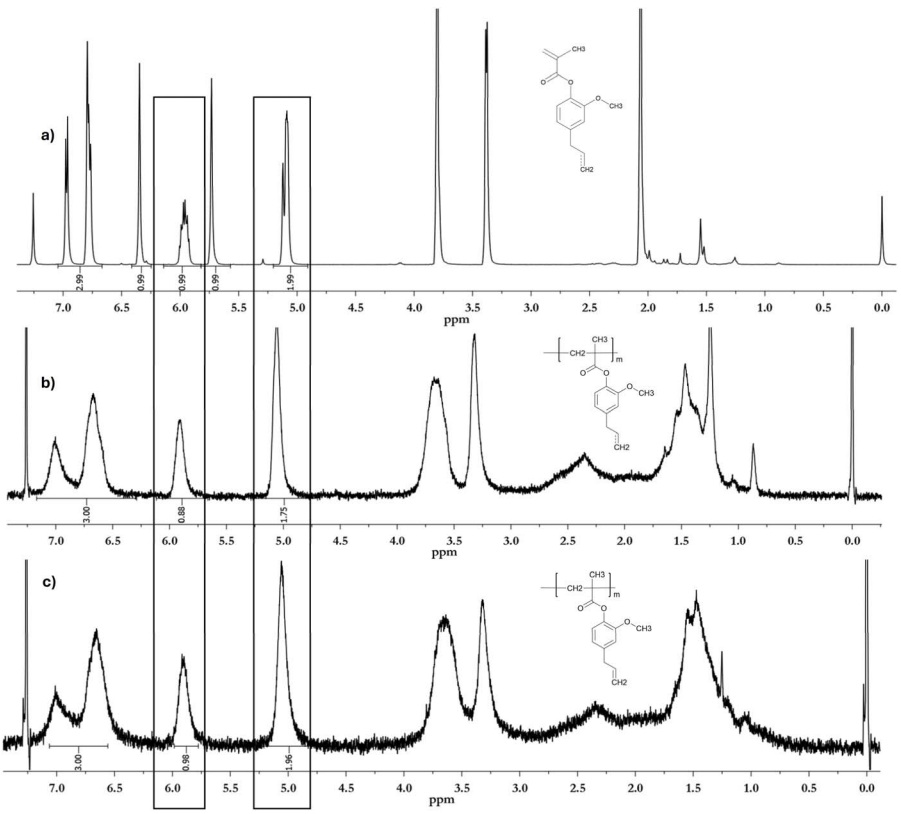

Fig. 5 ^{1}H NMR (500 MHz, CDCl3 + TMS, δ in ppm) for (a) methacrylate 1, (b) **poly-1** synthesized *via* Thio-RAFT, (c) **poly-1** synthesized by free-radical polymerisation/evaluation of the conversion of the C=C double bond in the allyl group.

of propagating radical chains are reported to promote extensive branching and crosslinking reactions. These side reactions can be suppressed by selecting low polymerisation temperatures.[48] This literature findings align well with the experimental results obtained in this study. By employing reduced reaction temperatures and a diluted polymerisation solution, branching reactions in **poly-1** could be minimized. When crosslinking is desired, RAFT polymerisation under concentrated conditions enables pronounced network formation, providing access to novel reaction pathways and structural architectures for monomer **1**. In this case, the goal was to suppress branching to the greatest possible extent. Nonetheless, due to ongoing side reactions, an increase in dispersity and a symmetrical shoulder in the GPC elugram were observed with progressing reaction time (Fig. 4F). This observation supports the theory that the initiation of polymer chains initially occurs exclusively at the methacrylate group, and that the reaction of the allyl group becomes more likely as the methacrylate concentration decreases. Notably, branching reactions were only initiated beyond a certain degree of polymerisation, suggesting that the allyl group becomes more reactive as methacrylate concentration declines. Despite this effect, the linear growth of molecular weight over time, characteristic of controlled polymerisation, is preserved. This confirms that free radical side reactions can be excluded, attributing shoulder formation solely to the particular reaction of the allyl C=C double bond. Analysis of the GPC elugram following free radical polymerisation of monomer **1** (Fig. S23) supports this conclusion. The appearance of the shoulder in the GPC elugram for RAFT polymerisation is accompanied by an increase in M_w/M_n over time, reaching a value of 1.5. However, this level of dispersity remains ensuring polymerisation proceeds under regulated conditions with predictable molecular weight distribution within the acceptable range for controlled polymerisations.[49,50] For comparison, the dispersity of **poly-1** obtained *via* free radical polymerization is 5.9 (Fig. S23). Further evidence from ^{1}H-NMR analysis confirmed an allyl conversion of approximately 15% (Fig. 7). Analysis of the reaction kinetics of the methacrylate group reveals that the free-radical polymerisation of monomer **1** exhibits only a slightly higher propagation rate compared to RAFT polymerisation. When compared with literature-reported rate constants for RAFT polymerisation of renewable aromatic methacrylates, the observed values are within a similar range. For instance, reaction rate constants between 0.21 and 0.29 have been reported for vanillin-, guaiacol-, or creosol-based methacrylates.[40]

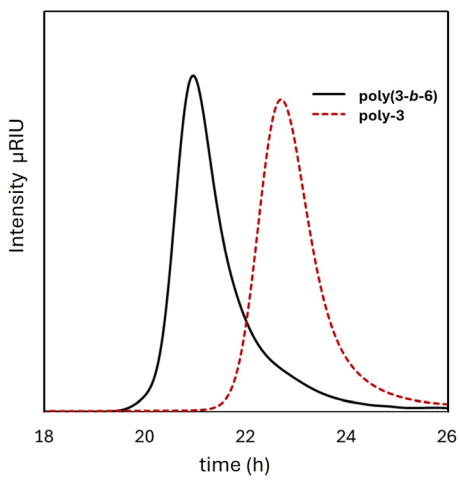

Fig. 6 GPC chromatogram **poly(3-*b*-6)** and **poly-3**.

Tailor-made RAFT-(diblock co)polymers based on renewable raw materials

Based on the previous detailed investigation of the monomers' reactivity *via* RAFT polymerisation, it has been confirmed that the synthesised biobased monomers **1** and **2** are suitable for polymerisation using RAFT, just as effectively as the selected conventional methacrylates **3** to **6**. The subsequent synthesis of structural heterogeneity block copolymers was successfully demonstrated with the polymer **poly(3-*b*-6)**. For a successful linkage to block copolymers, it is important to ensure that the conversion of the initially synthesised A-block does not exceed 98% before the dosing of the B-block begins. This promotes the formation of a short statistical transition segment and facilitates the effective coupling of the different methacrylates. To achieve this, a direct attachment of the B-block *via* an *in situ* one-pot reaction is recommended. Moreover, this approach helps prevent undesired termination reactions caused by oxygen intrusion at the chain ends of the A-block. Examination of the GPC elugram for **poly-(3-*b*-6)** (Fig. 6) after polymerisation reveals a shift towards a lower retention time, indicating successful chain extension. Additionally, the elugram displays a single narrow main peak without significant broadening or secondary elugrams, confirming uniform chain elongation due to the attached B-block (Fig. 6). After determining the appropriate polymerisation parameters, block copolymers were synthesised from the monomers 1 and 2, which are derived from renewable resources, as well as from structurally related commercial methacrylates. The fully biobased **poly(2-*b*-1)** exhibits a characteristic shoulder in the GPC trace (Fig. 7), which is attributed to the previously investigated crosslinking reaction involving the allyl double bond of eugenol (Fig. 4). A similar observation was made during the copolymerisation of **poly(6-*b*-1)**. Upon addition of monomer **1**, a bimodal elution profile becomes apparent, as seen in the GPC elugram (Fig. 7). However, as previously investigated, controlled RAFT polymerisation was still done. To further evaluate whether the polymers are indeed block copolymers despite the broad distribution observed in the GPC elugram, DOSY measurements were performed on **poly(2-*b*-1)** (Fig. S57), **poly(6-*b*-1)** (Fig. 8), and **poly(6-*b*-5)** (Fig. S56). The diffusion coefficients of the A-block and B-block are nearly identical, indicating a uniform molecular weight. For **poly(2-*b*-1)** and **poly(6-*b*-1)**, a distribution of molecular weights was observed, which can be attributed to the branching reaction of the allyl group in eugenol. As a result, block copolymers with varying molecular weights are formed, as also evident from the GPC analysis. Additionally, diffusion-filtered ^{1}H-NMR spectra of the thread polymers were

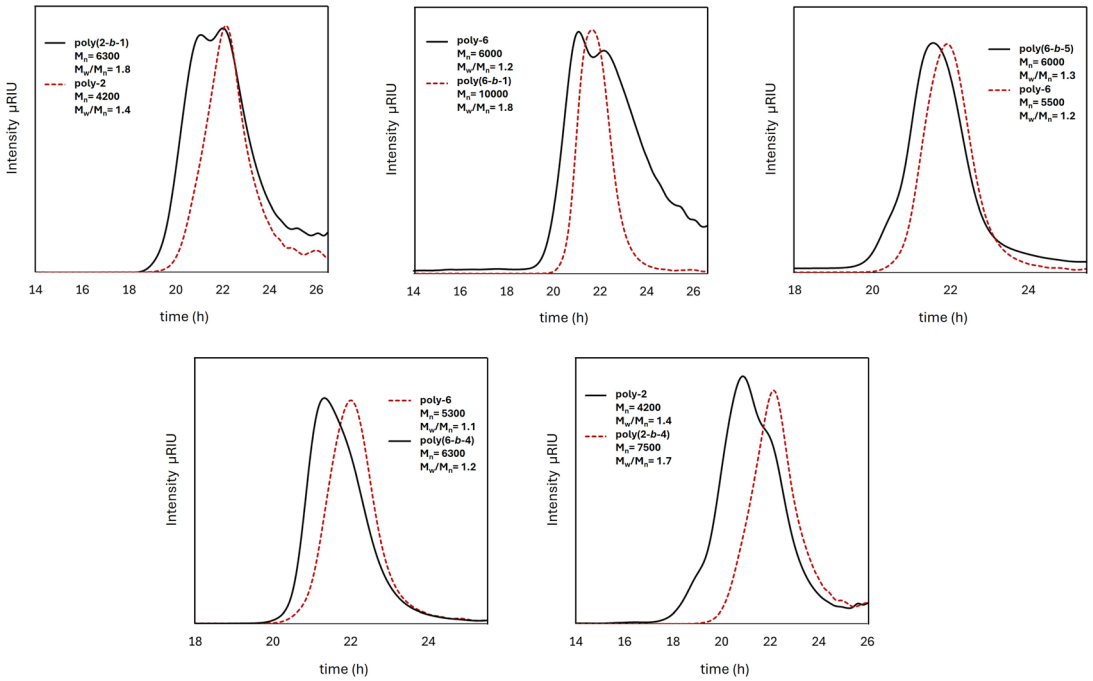

Fig. 7 GPC chromatogram synthesized block copolymers.

recorded. If the B-block had not been successfully attached to the A-block, its signals would be suppressed in the spectrum due to its low molecular weight. Experimental conditions were chosen to suppress signals of components with molecular weights below ~1800 g mol^{-1}. The presence of B-block signals in the spectrum thus confirms its covalent attachment to the A-block for **poly(6-*b*-1)** (Fig. 8), **poly(6-*b*-5)** (Fig. S56) and **poly(2-*b*-1)** (Fig. S57). This clearly confirms the block copolymer architecture. For the polymers **poly(6-*b*-5)** and **poly(6-*b*-4)**, derived from commercial monomers, well-defined block copolymers were obtained (Fig. 7). Monomer **5** was selected to investigate an additional aromatic anchoring group in comparison to monomer **1**. Interestingly, a slight shoulder formation was also observed in the GPC elution profile of **poly(2-*b*-4)** (Fig. 7), which correlates with the A-block. However, upon addition of the B-block, a pronounced shift of the main elugram toward higher molecular weights is evident. Since the amount of B-block monomer used would not be sufficient on its own to account for such high molecular weights, successful coupling of the B-block is confirmed. It is possible that undesired termination reactions occurred in this case, preventing activation of some A-block chains. This may also explain the slightly higher overall molecular weight of the resulting block copolymer compared to the theoretical expectation. This block copolymer nevertheless

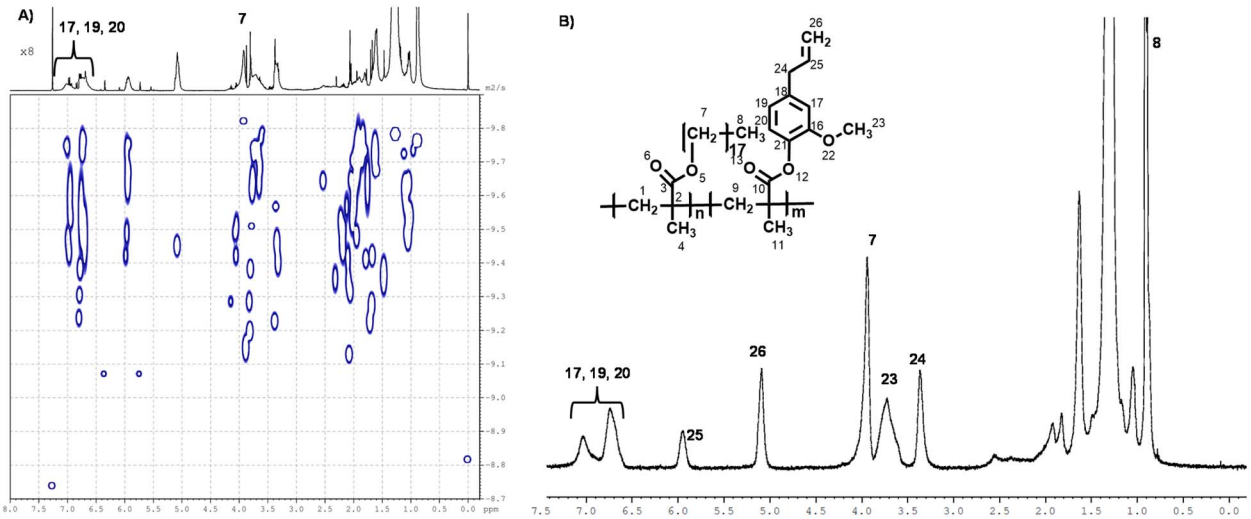

Fig. 8 (A) DOSY spectra and (B) diffusion-filtered ^{1}H-NMR spectra for **poly(6-*b*-1)**.

Table 3 Overview of concentration of reaction solution in PMA, conversion percentage (conv. %), theoretical molecular weight ($M_{n,th}$), actual molecular weight (M_n) and dispersity M_w/M_n, glass transition temperature (T_g), melting point (T_m), and thermal decomposition temperature (T_D)

Polymer	[M] (mol L^{-1})	Conv. (%)	$M_{n,th,A\text{-block}}$ (g mol^{-2})	$M_{n,A\text{-block}}$ (g mol^{-2})	$M_{n,th,A+B\text{-block}}$ (g mol^{-1})	$M_{n,A+B\text{-block}}$ (g mol^{-1})	M_w/M_n	T_m (°C)	T_{g1} (°C)	T_{g2} (°C)	T_D (°C)
poly(3-*b*-6)	7.3	97	5000	3500	10 000	7100	1.3	31.1	68.5	99.4	188.3
poly(2-*b*-1)	0.8	98	5000	4200	6500	6300[b]	1.8[b]	—	82.0	115.1	160.0
poly(6-*b*-1)	0.8	91	5000	6000	6500	10 000[b]	1.8[b]	31.2	107.8	—[a]	183.7
poly(6-*b*-5)	3.6	97	5000	5500	6500	6000	1.3	28.6	108.7	—[a]	179.2
poly(6-*b*-4)	4.8	95	5000	5300	6500	6300	1.2	26.3	85.5	—[c]	170.6
poly(2-*b*-4)	4.8	95	5000	4200	6500	7500	1.7	—	100.7	—[c]	163.1

[a] Too weakly pronounced to be definitively identified. [b] Consider properties of polymerisation of **1**. [c] Measurement not possible, as T_g is above T_D for RAFT polymer.

exhibits strong stabilizing properties as a dispersing additive in application tests. For all polymers, a clear chain extension was observed upon attachment of the desired B-block (Table 3). Narrow dispersity's within the range of controlled polymerisation were achieved, except for polymers containing monomer **1**, which can be attributed to the crosslinking reaction. The B-block was designed to remain significantly smaller than the nonpolar A-block. This structural characteristic is advantageous for applications as wetting and dispersing additives in nonpolar systems, as the polymer chains interact stabilizing with the solvent, while only the short polar B-block engages directly with the pigment.

Structural heterogeneity block copolymers for use as dispersing additives

The synthesised diblock copolymers, which were additionally characterised by FT-IR spectroscopy (Fig. 9C), were tested for their functionality as dispersing additives in a nonpolar system. A base formulation for an non polar system is used as suitable test environment. Aromatic moieties within the polymer backbone are known to facilitate specific interactions with organic pigments, likely through π–π stacking or hydrophobic interactions. In contrast, the incorporation of acidic functional groups is presumed to facilitate interactions with inorganic pigment particles. Additionally, the integration of nonpolar aliphatic chain segments is aimed at improving the compatibility and miscibility with the surrounding polymer matrix. The synthesized block copolymers were integrated into the respective formulations and compared with a reference sample and a negative control. Their rheological behaviour and particle size immediately after formulation (t_1) and following a storage period of two weeks at 60 °C (t_2) of the samples were measured. The increase in viscosity observed within the formulation is attributable to reagglomeration phenomena, which should be minimized to preserve formulation stability. For **poly(6-*b*-4)** and **poly(2-*b*-4)**, excellent results were achieved even after the storage period owing to the low viscosity within a range of 31 till 60 mPa*s, whereas the sample without additives exhibited a significant increase in viscosity of 127 mPa s immediately after production (*cf.* Fig. 9B). Ideally, the viscosity should be close to that of water and about 1 mPa s. In the formulation using carbon black, none of the samples exhibited a significant increase in viscosity (*cf.* Fig. 9A). To evaluate the effectiveness as a dispersing additive, particle size measurements were employed. In the sample containing **poly(6-*b*-1)**, a smaller particle size about 613 μm was measured before storage compared to the control sample. After storage, this value nearly doubled to 1123 μm (*cf.* Fig. 9A). This indicates that the system still requires further optimization to ensure long-term stabilization, even after storage. **Poly(2-*b*-1)** and **poly(6-*b*-5)** exhibited stable particle sizes before and after storage about a range of

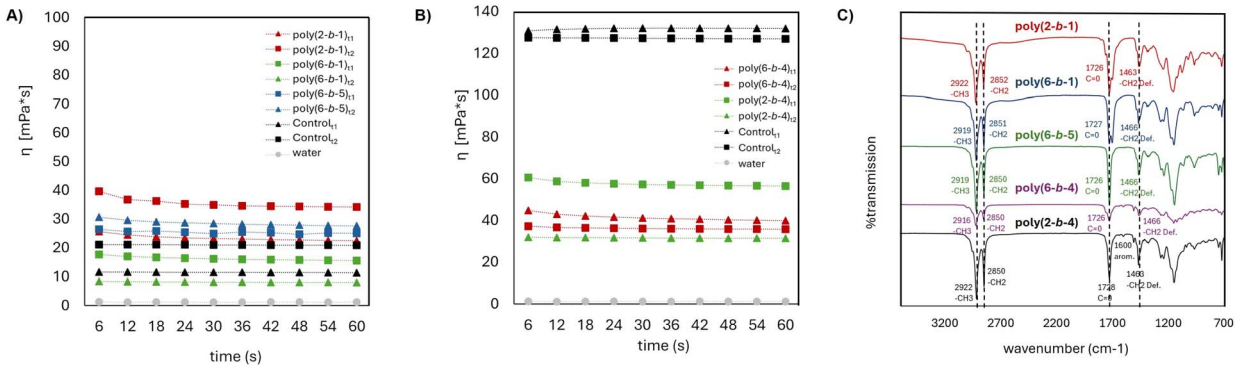

Fig. 9 Rheological measurements (A) system with carbon black (B) system with inorganic pigment (C) FT-IR spectra of synthesized block copolymers.

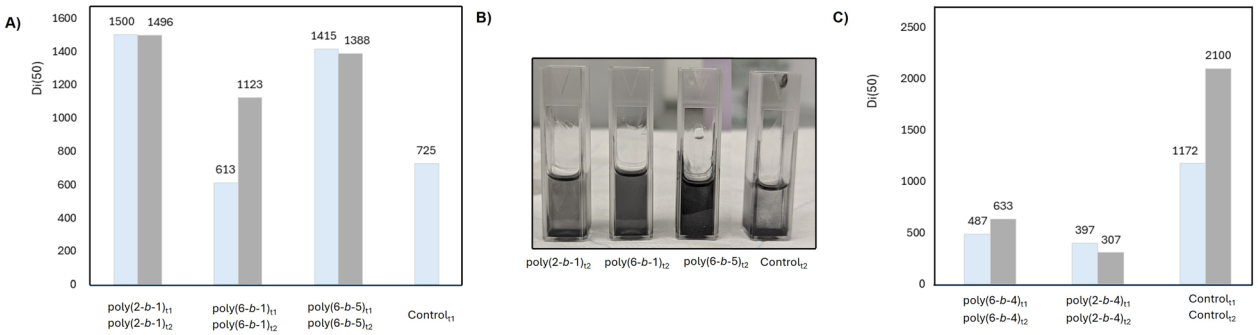

Fig. 10 Particle size measurements (A) system with carbon black (C) system with inorganic pigment (B) samples of the system containing carbon black after storage with varying degrees of sedimentation.

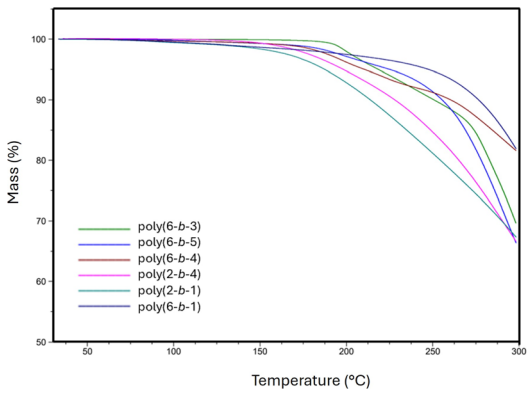

Fig. 11 TGA measurements of synthesized block copolymers.

1400 μm; although the average particle sizes of the test samples exceeded those of the control sample prior to storage. Complete sedimentation of pigments occurred in the control after storage, thereby preventing subsequent particle size analysis (Fig. 10B). In contrast, both **poly(6-*b*-1)** and **poly(6-*b*-5)** exhibited minimal sedimentation even after prolonged storage. Notably, **poly(6-*b*-5)** maintained the most consistent optical blackness over time (Fig. 9B). Submersible, a stabilizing effect of the pigments was observed for all employed diblock copolymers when compared to the control sample. Analysis of particle size in the samples containing **poly(6-*b*-4)** and **poly(2-*b*-4)** revealed excellent particle-stabilizing properties, likely attributable to strong interactions between methacrylic acid functionalities and the inorganic pigment surface (Fig. 10C). Moreover, the thermal stability of the synthesized block copolymers by their thermal decomposition temperature (T_D) was determined. This parameter is particularly relevant for assessing applicability in specific industrial applications. All samples exhibit thermal stability up to approximately 170 °C (Fig. 11). This level of thermal resistance appears sufficient for their application as dispersing additives in commercial systems.

Conclusions

The successful synthesis of structurally heterogeneous block copolymers *via* RAFT polymerisation was demonstrated, using methacrylates derived from renewable resources. This controlled radical polymerisation technology enabled precise molecular weight control, yielding low-dispersity polymers with well-defined architectures. During RAFT polymerisation, partial conversion of the allyl C=C double bond in monomer **1** was observed. This process is very unlikely under free radical polymerisation conditions. This crosslinking causes a shoulder formation in GPC elugrams, yet the process remained controlled RAFT polymerisation. This branching reaction can be suppressed or promoted by adjusting monomer concentration. This opens new possibilities for crosslinked polymers based on the renewable feedstock eugenol. The reaction kinetics of the biobased monomers were compared to methyl methacrylate and stearyl methacrylate at different concentrations. An increased reaction rate was observed for the aliphatic monomers under diluted conditions. However, at higher concentrations, this trend reversed, and these monomers exhibited a reduced reaction rate. Thermal characterization revealed that the decomposition behaviour of the polymers falls within a suitable range for many industrial applications. Previous studies demonstrated that monomer **6** can be successfully replaced with lauryl methacrylate, resulting in an optimized block copolymer. This confirms that further variation of nonpolar monomers remains a viable strategy for future optimization. The synthesised block copolymeres were evaluated for their suitability as dispersing additives in nonpolar systems. Notably, **poly(6-*b*-4)** and **poly(2-*b*-4)** exhibited excellent pigment stabilization properties, particularly for inorganic pigments. **Poly(6-*b*-1)** also showed strong stabilizing performance, even after extended storage. These findings indicate that the synthesized polymers, based on bio-derived raw materials, are well-suited for use as dispersing additives. This approach supports the principles of a circular economy and reduces reliance on primary raw materials, thereby promoting more efficient resource utilization and minimizing environmental impact.[10,51,52] One limitation, however, is that direct extraction of oleyl alcohol from rapeseed oil competes with the food industry. Encouragingly, increasing efforts are being made to develop processes for recycling used cooking oils to synthesize oleyl alcohol, which may help mitigate this issue. Furthermore, recent advances in chemical technology, microbial fermentation, and thermal catalysis have enabled the bio-based

production of methacrylic acid from glucose *via* the intermediate citramalic acid.[53] This allows for the replacement of fossil-derived methacrylic acid. Consequently, the diblock polymers **poly(2-*b*-4)** and **poly(2-*b*-1)** synthesized in this study can be designed to be fully bio-based.

Conflicts of interest

There are no conflicts to declare.

Data availability

The raw data required to produce these findings cannot be shared at this time as the data also forms part of an ongoing study.

Supplementary information: ^{1}H NMR spectra of synthesized compounds, GPC elugrams of synthesized polymers, DSC curves of polymers, TGA curves of homopolymers, FT-IR spectra of synthesized polymers, DOSY and diffusion filtered ^{1}H-NMR spectra. See DOI: **https://doi.org/10.1039/d5ra06866e**.

Acknowledgements

The authors would like to express their sincere gratitude to the entire analytical team at BYK-Chemie, Wesel, Germany, as well as the end-use application team, for their dedicated collaboration and valuable technical support throughout the course of this study. Moreover, we gratefully acknowledge ALTANA AG for awarding the ALTANA Institute Project, which enabled this research.

References

1 H. Baumann, M. Bühler, H. Fochem, F. Hirsinger, H. Zoebelein and J. Falbe, *Angew Chem. Int. Ed. Engl.*, 1988, **27**, 41–62.
2 S. Molina-Gutierrez, V. Ladmiral, R. Bongiovanni, S. Caillol and P. Lacroix-Desmazes, *Ind. Eng. Chem. Res.*, 2019, **58**, 21155–21164.
3 S. Boner, K. Parkatzidis, N. D. A. Watuthanthrige and A. Anastasaki, *Eur. Polym. J.*, 2024, **205**, 112721.
4 V. K. Thakur, M. K. Thakur, P. Raghavan and M. R. Kessler, *ACS Sustain. Chem. Eng.*, 2014, **2**, 1072–1092.
5 M. A. R. Meier, J. O. Metzger and U. S. Schubert, *Chem. Soc. Rev.*, 2007, **36**, 1788–1802.
6 Z. Wang, M. S. Ganewatta and C. Tang, *Prog. Polym. Sci.*, 2020, **101**, 101197.
7 A. Vitale, S. Molina-Gutiérrez, W. S. J. Li, S. Caillol, V. Ladmiral, P. Lacroix-Desmazes and S. Dalle Vacche, *Materials*, 2022, **15**, 339.
8 M. Di Consiglio, E. Sturabotti, B. Brugnoli, A. Piozzi, L. M. Migneco and I. Francolini, *Polym. Chem.*, 2023, **14**, 432–442.
9 University of Delaware, *US Pat.*, US20140275435, 2014.
10 N. Wu, Z. Demchuk, A. Voronov and G. Pourhashem, *J. Cleaner Prod.*, 2021, **286**, 124939.
11 University of Delaware, *US Pat.*, US20190144590, 2019.
12 M. Shibata, Y. Itakura and H. Watanabe, *Polym. J.*, 2013, **45**, 758–765.
13 B. Domnich, H. Lynch and A. Voronov, *Int. J. Adhes. Adhes.*, 2024, **128**, 103574.
14 P. Saindane and R. N. Jagtap, *Prog. Org. Coat.*, 2015, **79**, 106–114.
15 L. Zhang, J. Ma, B. Lyu, Y. Zhang, V. K. Thakur and C. Liu, *Green Chem.*, 2021, **23**, 7576–7588.
16 F. L. Hatton, *Polym. Chem.*, 2020, **11**, 220–229.
17 C. Voirin, S. Caillol, N. V. Sadavarte, B. V. Tawade, B. Boutevin and P. P. Wadgaonkar, *Polym. Chem.*, 2014, **5**, 3142–3162.
18 M. Kepkow, M. Heinz, L. Omerbegovic, S. Schillat, B. Strehmel and V. Strehmel, *Sustainable Chem. Pharm.*, 2025, **44**, 101961.
19 Z. Demchuk, A.-S. Mora, S. Choudhary, S. Caillol and A. Voronov, *Ind. Crops Prod.*, 2021, **162**, 113237.
20 C. Mabille, V. Schmitt, P. Gorria, F. Leal Calderon, V. Faye, B. Deminière and J. Bibette, *Langmuir*, 2000, **16**, 422–429.
21 S. E. Shim, H. Lee and S. Choe, *Macromolecules*, 2004, **37**, 5565–5571.
22 K. Kataoka, A. Harada and Y. Nagasaki, *Adv. Drug Delivery Rev.*, 2012, **64**, 37–48.
23 A. W. York, S. E. Kirkland and C. L. McCormick, *Adv. Drug Delivery Rev.*, 2008, **60**, 1018–1036.
24 M. L. Adams, A. Lavasanifar and G. S. Kwon, *J. Pharm. Sci.*, 2003, **92**, 1343–1355.
25 H. Buksa, E. C. Johnson, D. H. H. Chan, R. J. McBride, G. Sanderson, R. M. Corrigan and S. P. Armes, *Biomacromolecules*, 2024, **25**, 2990–3000.
26 J. Yang, Y. Mu and X. Li, *Mater. Lett.*, 2022, **322**, 132493.
27 T. Brock, M. Groteklaes, P. Mischke and B. Strehmel, *Lehrbuch der Lacktechnologie*, Vincentz Network, Hannover, Germany, 2017.
28 S. Perrier, *Macromolecules*, 2017, **50**, 7433–7447.
29 A. J. Convertine, B. S. Sumerlin, D. B. Thomas, A. B. Lowe and C. L. McCormick, *Macromolecules*, 2003, **36**, 4679–4681.
30 A. B. Lowe and C. L. McCormick, *Prog. Polym. Sci.*, 2007, **32**, 283–351.
31 A.-C. Lehnen, J. A. M. Kurki and M. Hartlieb, *Polym. Chem.*, 2022, **13**, 1537–1546.
32 Y. Wan, W. Zhao, H. Zhao, M. Zhou, J. He and Y. Zhang, *Macromolecules*, 2023, **56**, 7763–7770.
33 G. Moad, *Polym. Chem.*, 2017, **8**, 177–219.
34 A. E. Smith, X. Xu and C. L. McCormick, *Prog. Polym. Sci.*, 2010, **35**, 45–93.
35 C. Barner-Kowollik, M. Buback, B. Charleux, M. L. Coote, M. Drache, T. Fukuda, A. Goto, B. Klumperman, A. B. Lowe, J. B. McLeary, G. Moad, M. J. Monteiro, R. D. Sanderson, M. P. Tonge and P. Vana, *J. Polym. Sci., Part A: Polym. Chem.*, 2006, **44**, 5809–5831.
36 M. Balarezo, F. Coumes and F. Stoffelbach, *Polym. Chem.*, 2022, **13**, 6525–6533.
37 I. Chaduc, W. Zhang, J. Rieger, M. Lansalot, F. D'Agosto and B. Charleux, *Macromol. Rapid Commun.*, 2011, **32**, 1270–1276.

38 K. Pramod, S. H. Ansari and J. Ali, *Nat. Prod. Commun.*, 2010, **5**, 1999–2006.
39 S. Molina-Gutierrez, S. D. Vacche, A. Vitale, V. Ladmiral, S. Caillol, R. Bongiovanni and P. Lacroix-Desmazes, *Molecules*, 2020, **25**, 3444.
40 A. L. Holmberg, M. G. Karavolias and T. H. Epps, *Polym. Chem.*, 2015, **6**, 5728–5739.
41 K. Kubo, A. Goto, K. Sato, Y. Kwak and T. Fukuda, *Polymer*, 2005, **46**, 9762–9768.
42 L. Spagnola, E. S. Daniels, V. L. Dimonie, M. S. El-Aasser and A. Klein, *PMSE Prepr.*, 2008, **99**, 752–753.
43 S. Warwel, G. Steinke and M. R. Klass, *Biotechnol. Tech.*, 1996, **10**, 283–286.
44 K. Matyjaszewski and J. Spanswick, *Mater. Today*, 2005, **8**, 26–33.
45 M. H. Keshavarz, K. Esmaeilpour and H. Taghizadeh, *J. Therm. Anal. Calorim.*, 2016, **126**, 1787–1796.
46 R. Y. F. Liu, T. E. Bernal-Lara, A. Hiltner and E. Baer, *Macromolecules*, 2005, **38**, 4819–4827.
47 Y. Gao, F. R. Kogler and U. Schubert, *J. Polym. Sci., Part A: Polym. Chem.*, 2005, **43**, 6586–6591.
48 A. Vittore, O. Santoro, M. Candida, S. Vaghi, S. Pragliola, M. Mella and L. Izzo, *Polymer*, 2025, **324**, 128228.
49 L. Zhang, Z. Zhang and M. Chen, *Chem. Res. Chin. Univ.*, 2023, **39**, 816–821.
50 J.-Y. Wang, Y.-Y. Ni, J.-N. Cheng, L.-F. Zhang and Z.-P. Cheng, *Chin. J. Polym. Sci.*, 2021, **39**, 1155–1160.
51 A. Orjuela and J. Clark, *Curr. Opin. Green Sustainable Chem.*, 2020, **26**, 100369.
52 A. Kohut, Z. Demchuk, K. Kingsley, S. Voronov and A. Voronov, *Eur. Polym. J.*, 2018, **108**, 322–328.
53 Y. Wu, M. Shetty, K. Zhang and P. J. Dauenhauer, *ACS Eng. Au*, 2022, **2**, 92–102.